Electronic Supplementary Material (ESI) for Nanoscale.

Ligand effect on size, valence state and red/near infrared photoluminescence of bidentate thiol gold nanoclusters - Supporting information

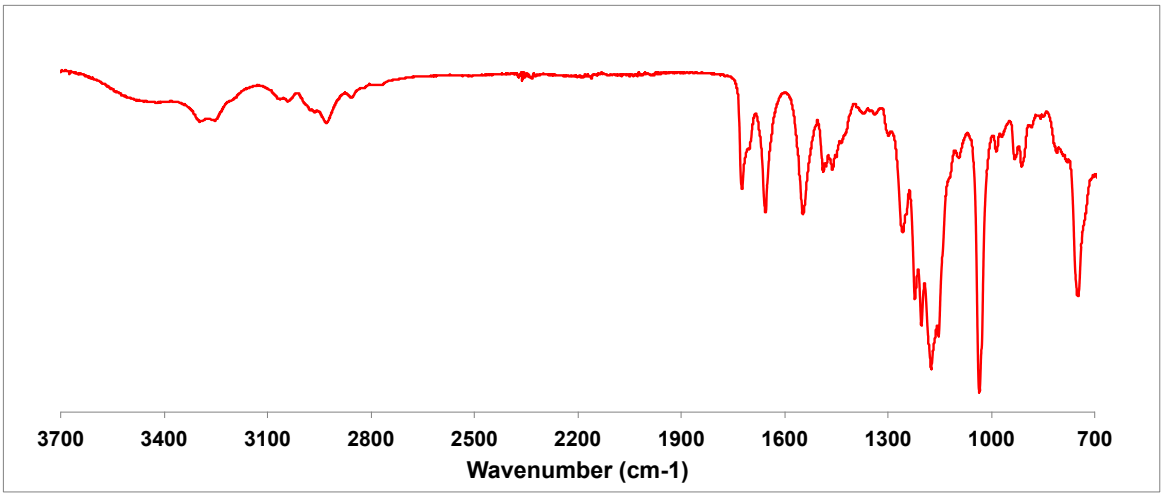

Fig. S1. Infrared spectrum of Zw between 700 and 3700 cm^{-1}. Characteristic peaks of Zw : ν=1654 cm^{-1} (s, ν (amide C=O)); ν=1544 cm^{-1} (m, ν(amide N-H)); ν=1180 cm^{-1} (m, ν (sulfonate S=O)); ν=1037 cm^{-1} (s, ν (aliphatic amine C-N)).

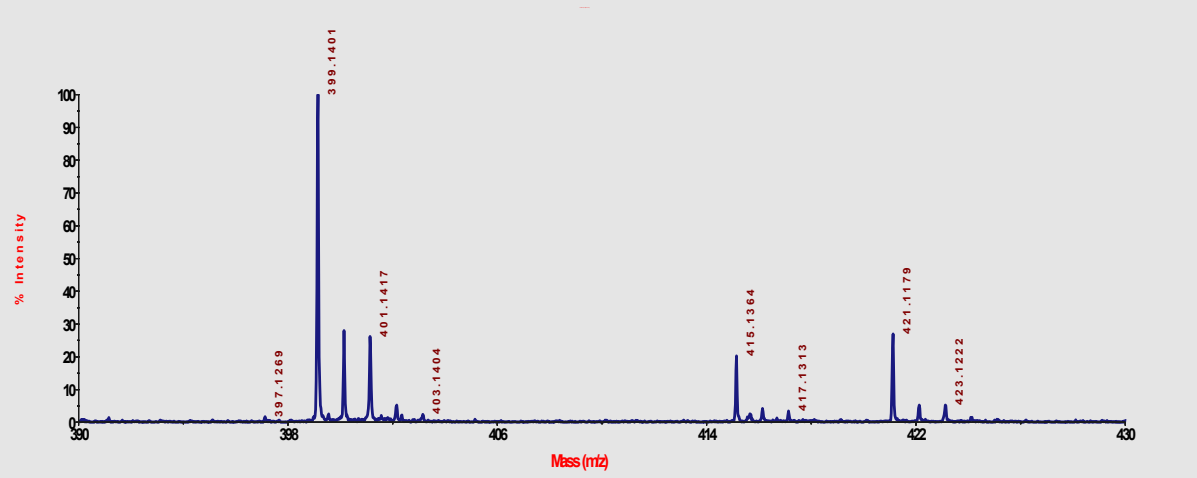

Fig. S2. Maldi/Tof in reflective mode of Zw with the matrix α-Cyano-4-hydroxycinnamic acid (**CHCA**) of Zw calculated for $C_{15}H_{30}N_2O_4S_3$ at 398.1 $[Zw+H]^+$ found at 399.1.

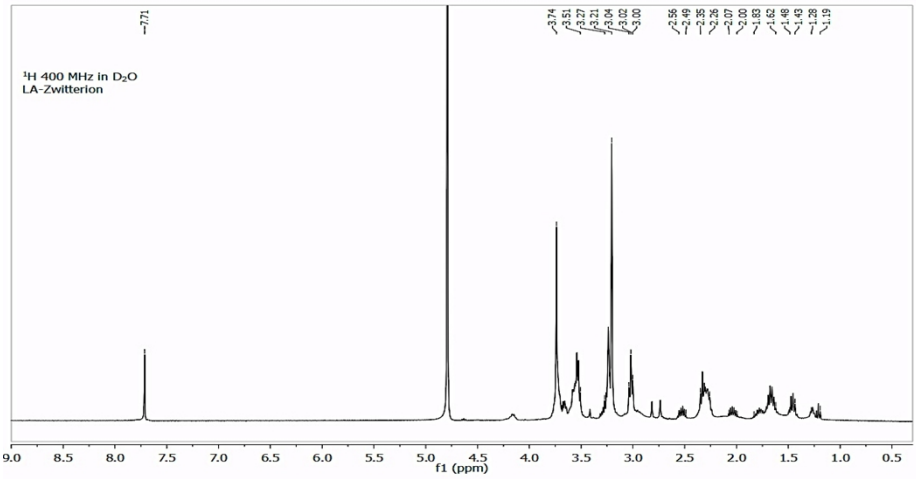

Fig. S3. ^{1}H NMR (D_2O, 400MHz) of Zw. δ[ppm]: 3.66-3.75 (m, 4H), 3.46-3.55 (m, 4H), 3.14-3.29 (m, 8H), 2.96-3.01 (t, 2H J= 6Hz, 2.44-2.54 (m, 1H), 2.19-2.32 (m, 4H), 1.94-2.05 (m, 1H), 1.55-1.79 (m, 4H), 1.36-1.46 (m, 2H).

Table S1. Determination of the weight loss of AuZw samples prepared at different Au:Zw ratio.

	Weight loss between 30°C - 500°C (wt%)	**Weight loss at 800°C (wt%)**
Zw	73.3	96.1
AuZw 1:1	32.3	53.0
AuZw 1:2	40.7	57.5
AuZw 1:3	42.2	61.0
AuZw 1:5	45.2	65.7
AuZw 1:10	61.7	81.6
AuZw 1:20	67.0	89.0
AuZw 1:40	68.4	89.4

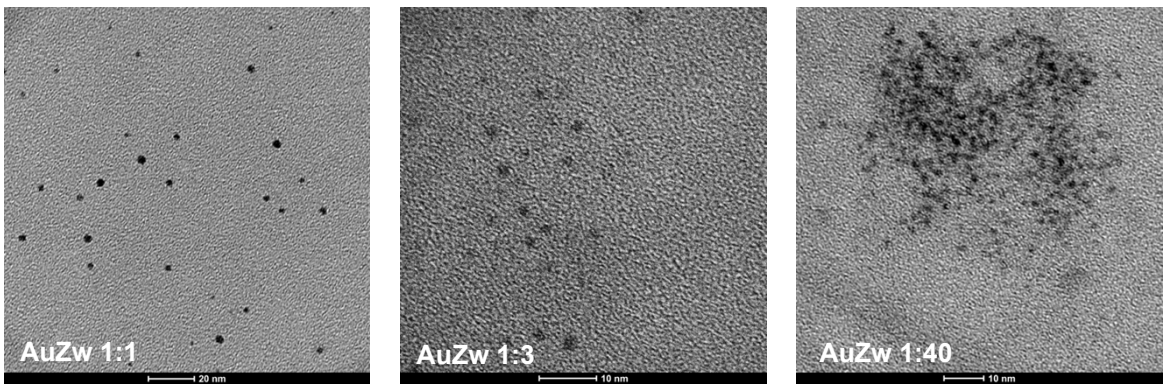

Fig. S4. Transmission electron microscope (TEM) images of AuZw 1:1, AuZw 1:3 and AuZw 1:40. The sample AuZw 1:1 presents some polydispersity with particle size above 2 nm.

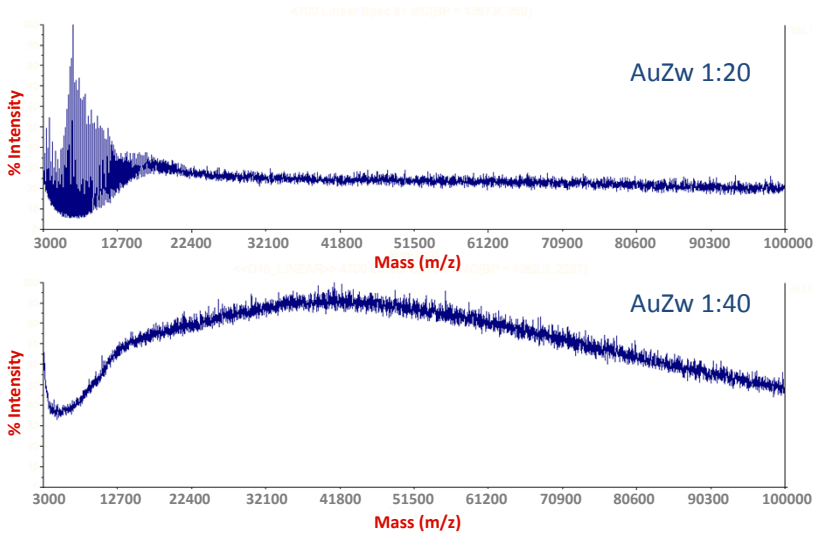

Fig. S5. MALDI/TOF in linear positive mode of AuZw 1:20 and AuZw 1:40 using CHCA as matrix. Measurements show the shift of the band corresponding to the Au NCs associated to the ligand to the high molecular weight. The high contribution of the organic moiety for AuZw 1:40 prevents the ionization of the fragmented AuNCs.

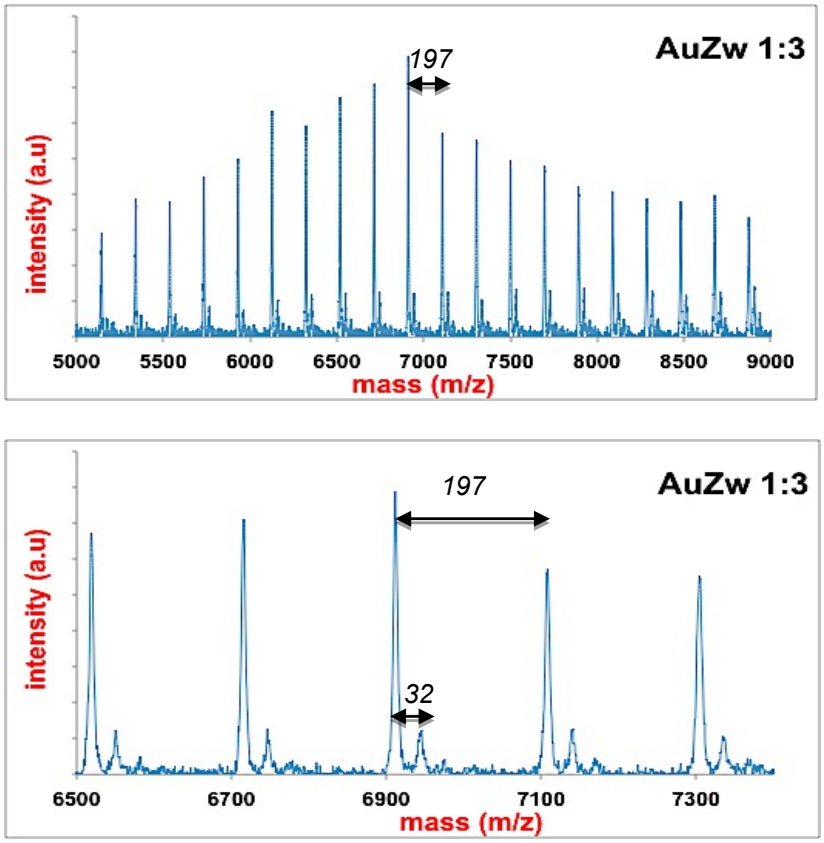

Fig. S6. MALDI/TOF in linear positive mode of AuZw 1:3 using CHCA as matrix. The shift of mass m/z= 197 and m/z= 32 correspond to the fragmentation of thiol gold nanoclusters.

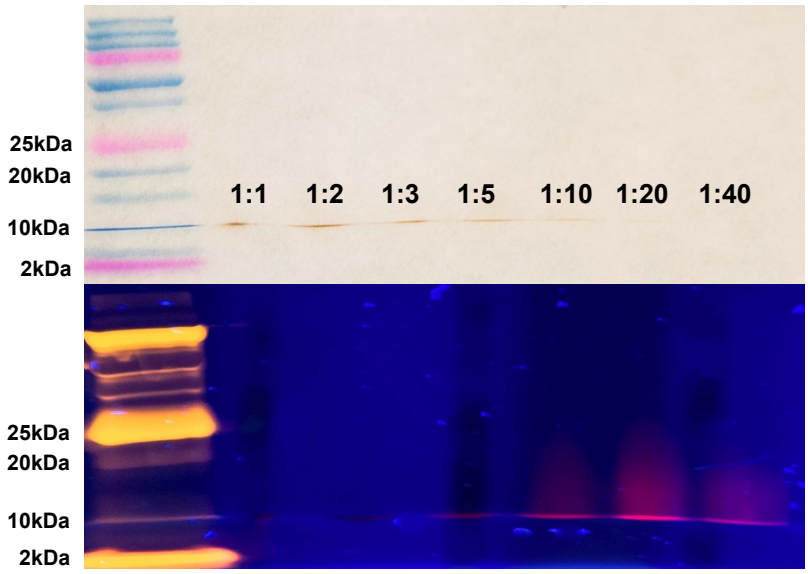

Fig. S7. PAGE electrophoresis of AuZw with Au:Zw = 1:1; 1:2; 1:3; 1:5; 1:10; 1:20 and 1:40. AuZw with ratio Au:R (R< 5) do not fluoresce in the visible range.

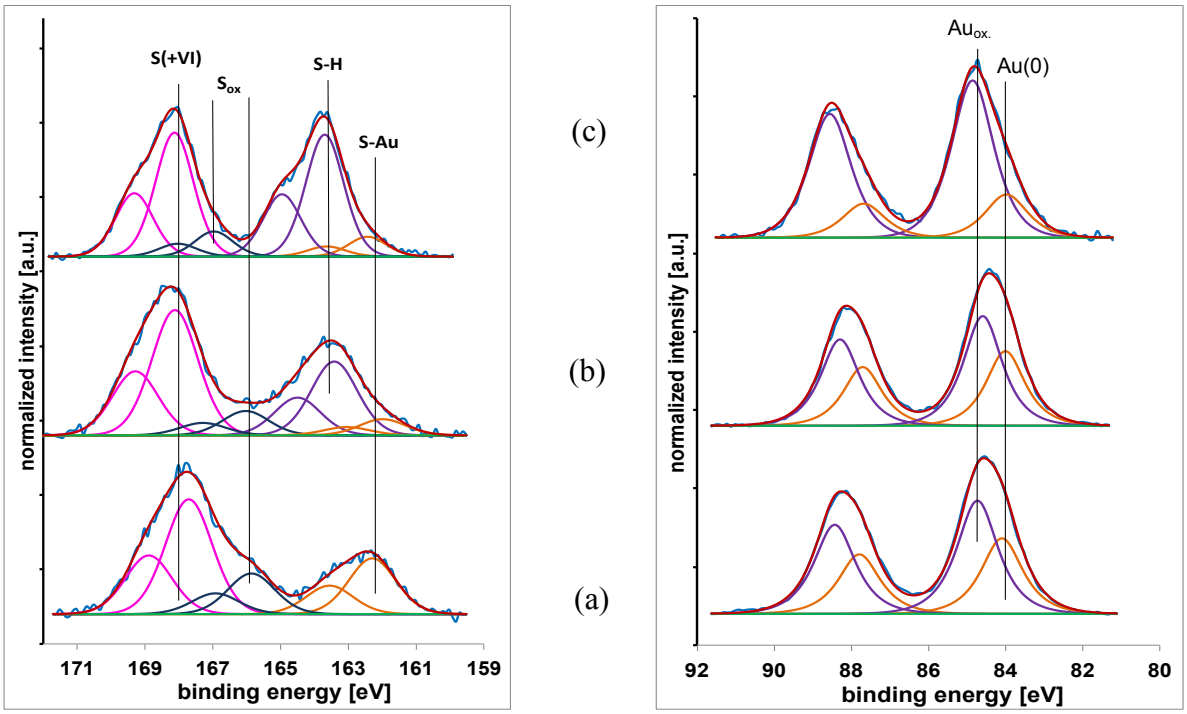

Fig. S8. XPS spectra of S 2p (left side) and Au 4f (right side) of AuZw 1:1 (a), AuZw 1:3 (b), and AuZw 1:20 (c). Au4f$_{7/2}$ can be deconvoluted in two distinct bands: one located at 84.0 eV corresponding to Au(0) and the second one at 84.7 eV, which can be attributed to partially-oxidized gold atoms. The binding energies of S 2p$_{3/2}$ at 162.0 eV, 163.5 eV, 165.0 eV and 168.0 eV are assigned to metal-ligand, sulfur bound to hydrogen/carbon,

partially oxidized sulfur (with a degree IV) and fully oxidized sulfur, respectively. Spectra of S 2p enable to see the increase of the peak at 163.5 eV related to S-H (purple line) when the ratio Au:Zw increases from 1:1 to 1:20.

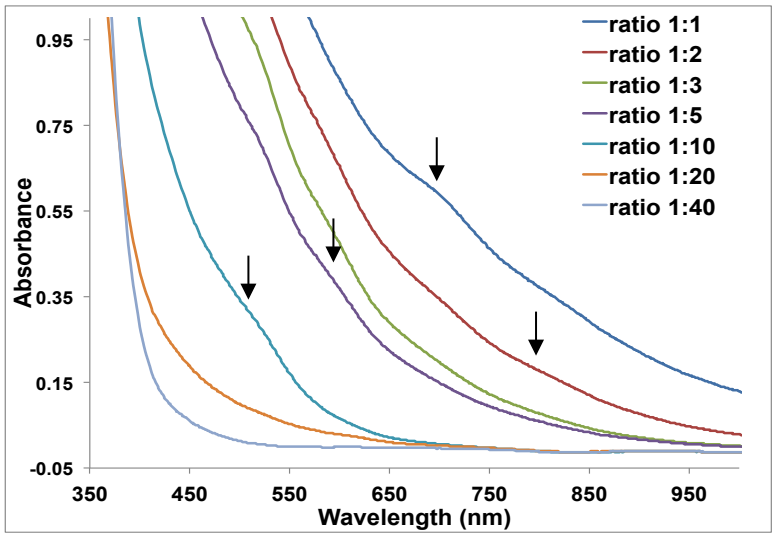

Fig. S9. Absorbance spectra of AuZw solutions at different ratio Au:Zw. (Gold concentration = 500 µg/mL). Arrows indicate the weak absorption bands observed at 510 nm (2.43 eV), 590 nm (2.10 eV), 700 nm (1.77 eV) and 820 nm (1.51 eV).

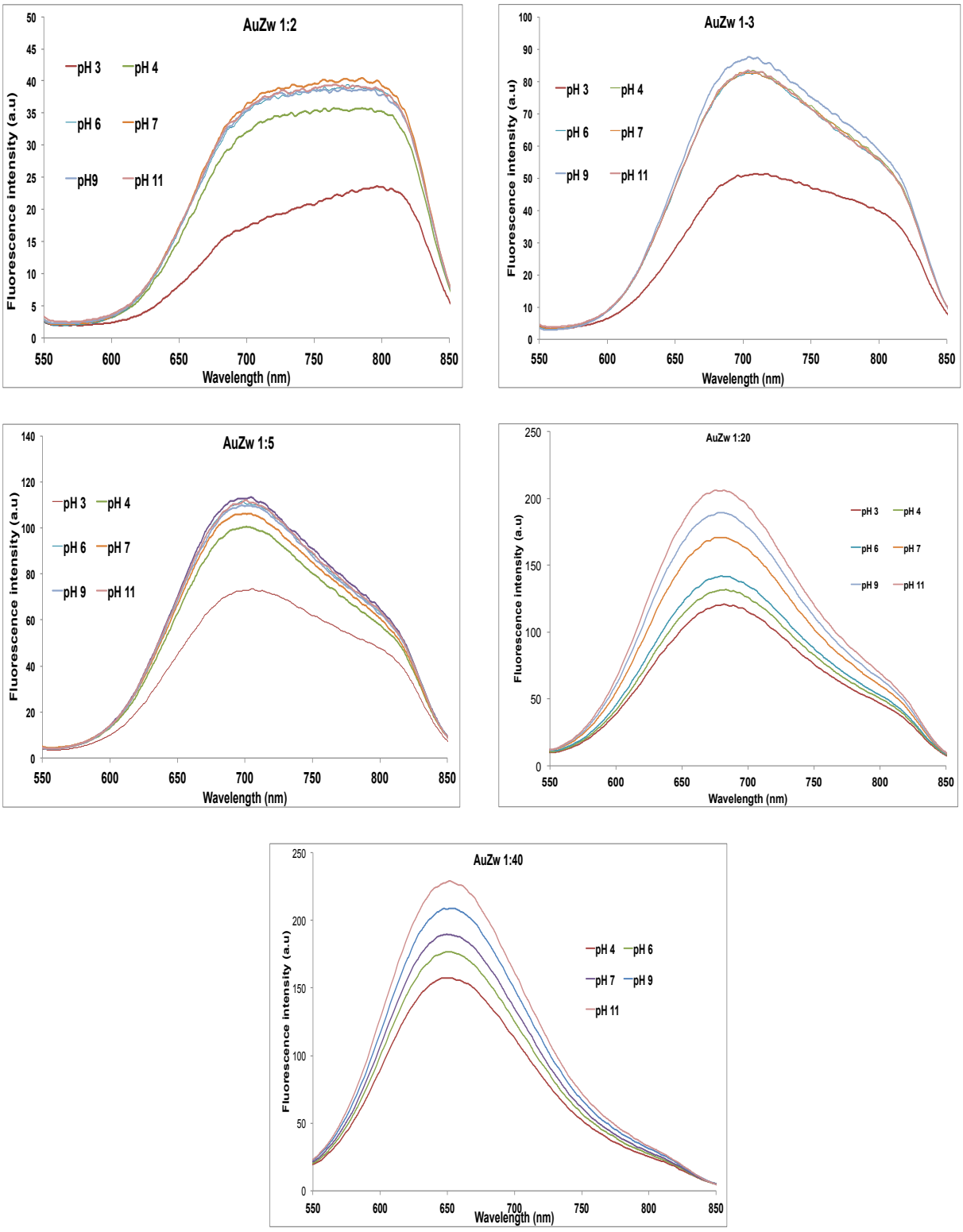

Fig. S10. Fluorescence emission of AuZw at different pH between 3 and 11. Excitation at $\lambda_{exc.}$= 450 nm. Fluorescence measurements of AuZw 1:1 were not performed at different pH due to weak signal intensities.

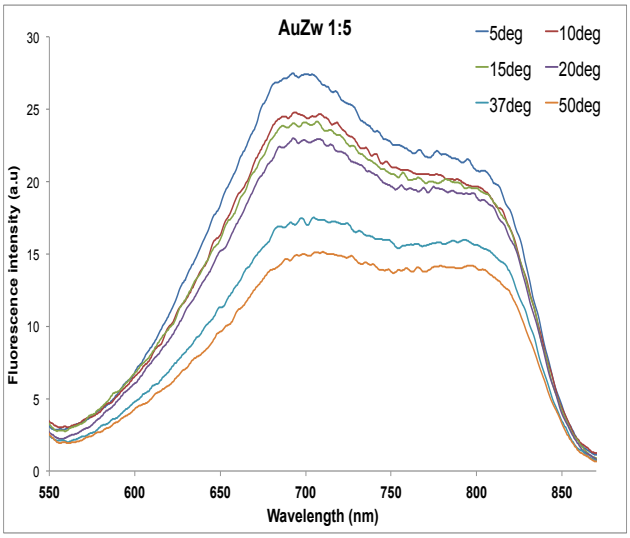

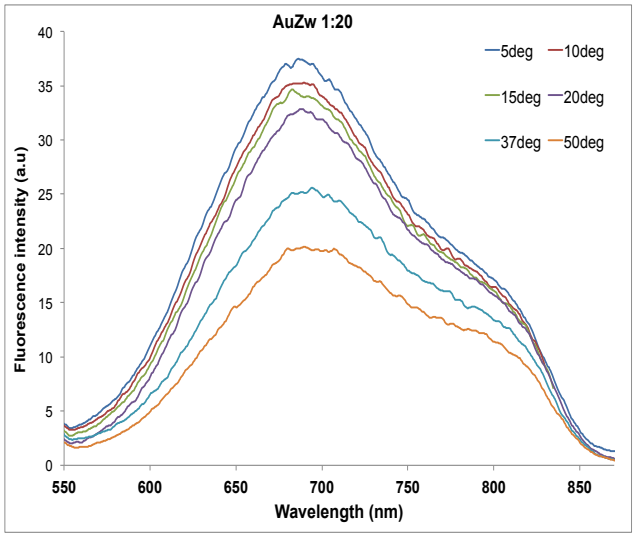

Fig. S11. Fluorescence emission of different AuZw samples at 5 and 50°C. Excitation at λ= 450 nm.

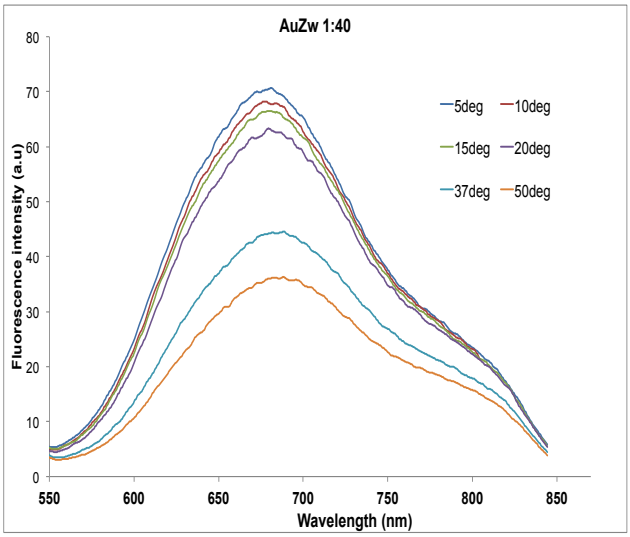

Table S2. PL quantum yields of different AuZw ratios at comparative method determined by Rhodamine 6G using (QY=0.95 in EtOH) with O.D. = 0.1.

	Φ (%)
AuZw 1:1	0.8
AuZw 1:2	1.1
AuZw 1:3	1.2
AuZw 1:5	5.5
AuZw 1:10	5.8
AuZw 1:20	7.9
AuZw 1:40	15.1

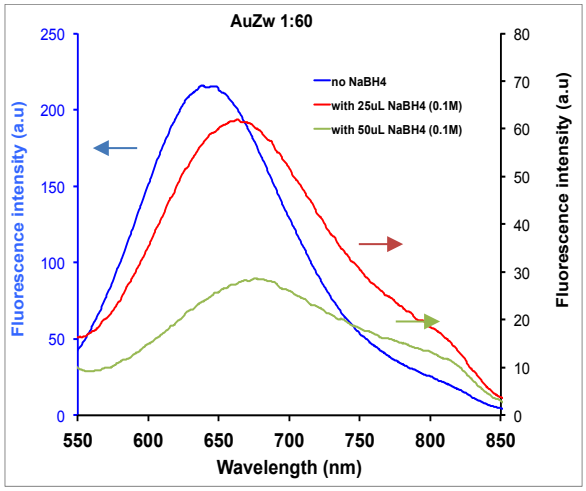

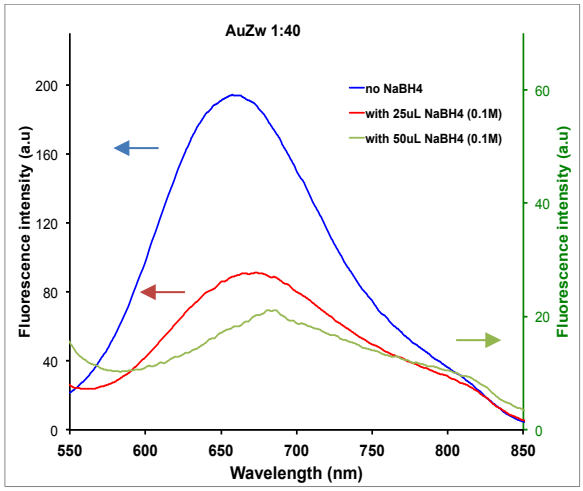

Fig. S12. PL e ı:Zw 1:40 and AuZw 1:3 after two cy

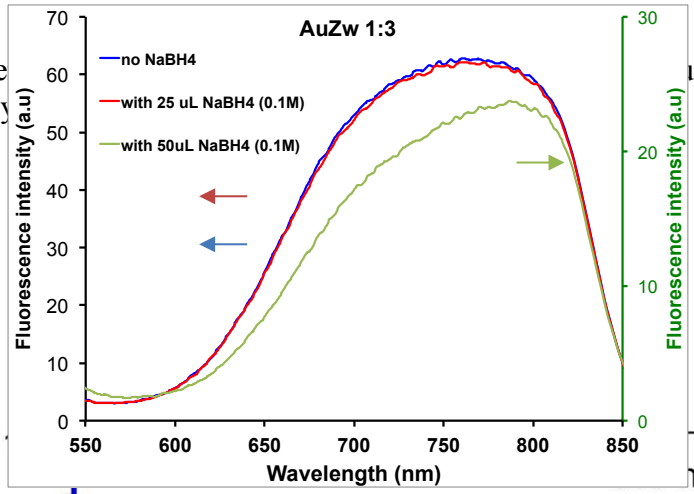

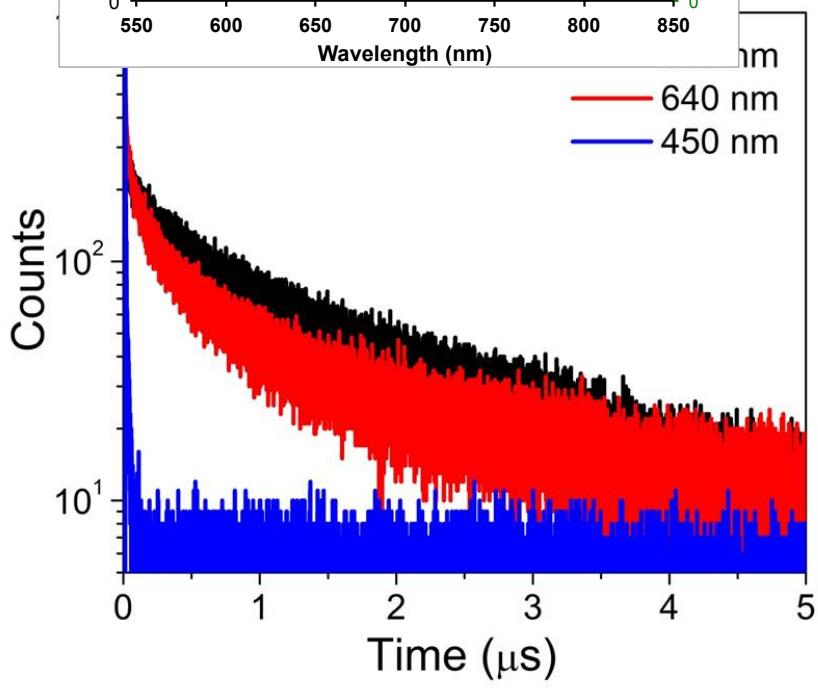

Figure S13. PL decay curves of AuZw 1:5 at different emission wavelengths using the same excitation wavelength of 405 nm. The red/NIR decay curves (at 640 nm and 800 nm) show significantly longer (1 to 3 orders of magnitude) decays than the visible decay curve (450 nm). .

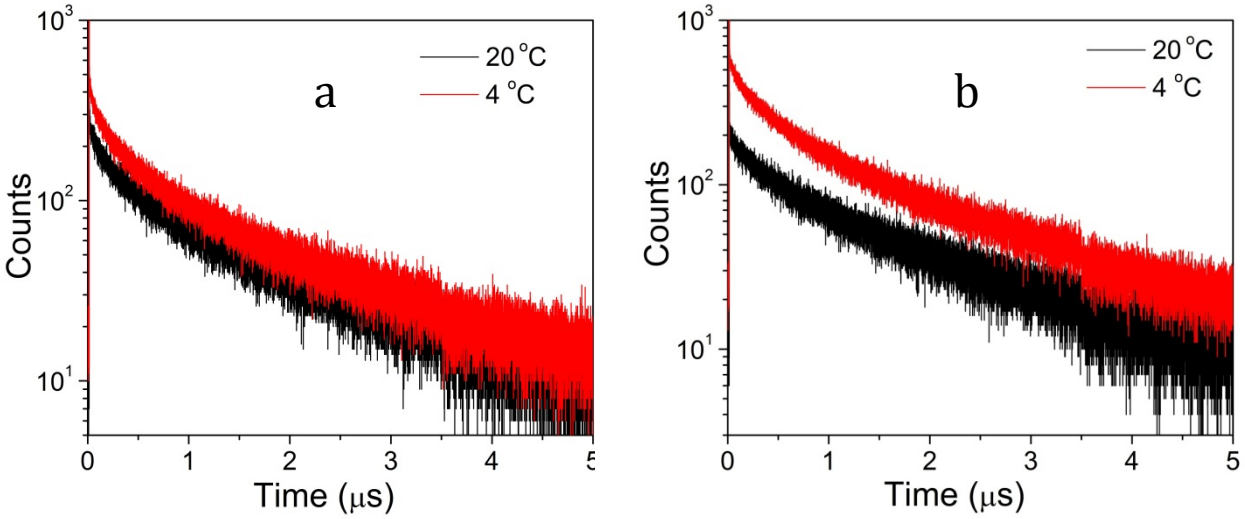

Fig. S14. PL decay curves for (a) AuZw 1:5 and (b) AuZw 1:40 recorded at 20 °C (black) and 4 °C (red). $\lambda_{exc.}$ = 405 nm, $\lambda_{em.}$ = 800 nm.

Table S3. PL decaytimes τ_1 and τ_2 and their amplitudes A_1 and A_2 (fractions a_1 and a_2 in paraphrases) and intensity and amplitude averaged decay times ($\tau_{int}=(A_1\tau_1^2+A_2\tau_2^2)/(A_1\tau_1+A_2\tau_2)$ and $\tau_{amp}=(A_1\tau_1+A_2\tau_2)/(A_1+A_2)$) of AuZw 1:5 and 1:40 at different temperatures and emission wavelengths using 405 nm as excitation wavelength.

λ [nm]	T (°C)	τ_1 [μs]	A_1	τ_2 [μs]	A_2	τ_{int} [μs]	τ_{amp} [μs]
640 nm	5	1.3	65 (38%)	0.2	106 (62%)	1.1	0.6
	10	1.4	56 (38%)	0.2	91 (62%)	1.2	0.6
	20	1.2	53 (32%)	0.1	113 (68%)	1	0.5
	37	1	75 (27%)	0.1	198 (73%)	0.8	0.4
700 nm	5	1.5	127 (45%)	0.2	155 (55%)	1.3	0.8
	10	1.5	120 (45%)	0.2	148 (55%)	1.3	0.8
	20	1.4	102 (42%)	0.2	141 (58%)	1.2	0.7
	37	1.2	158 (36%)	0.2	284 (64%)	1	0.6
800 nm	5	1.6	112 (53%)	0.3	100 (47%)	1.5	1
	10	1.6	95 (48%)	0.2	101 (52%)	1.4	0.9
	20	1.4	103 (45%)	0.2	128 (55%)	1.2	0.8
	37	1.3	166 (41%)	0.2	241 (59%)	1.1	0.6
700 nm	5	1.6	195 (52%)	0.2	177 (48%)	1.4	0.9
	10	1.6	141 (53%)	0.3	126 (47%)	1.4	1
	20	1.3	151 (46%)	0.2	180 (54%)	1.2	0.7
	37	1.2	240 (42%)	0.2	337 (58%)	1	0.6
800 nm	5	1.7	105 (57%)	0.3	78 (43%)	1.6	1.1
	10	1.6	87 (55%)	0.3	70 (45%)	1.5	1
	20	1.5	91 (48%)	0.3	98 (52%)	1.3	0.8
	37	1.3	155 (45%)	0.2	187 (55%)	1.1	0.7

AuZw 1:40

Error on the fluorescence lifetimes: ***±0.1μs***